

Quantum Many-Body Scarring in 2 + 1D Gauge Theories with Dynamical Matter

Jesse Osborne¹,^{*} Ian P. McCulloch²,^{*} and Jad C. Halimeh^{3,4,5,*}

¹*School of Mathematics and Physics, The University of Queensland, St. Lucia, QLD 4072, Australia*

²*Department of Physics, National Tsing Hua University, Hsinchu 30013, Taiwan*

³*Department of Physics and Arnold Sommerfeld Center for Theoretical Physics (ASC),*

Ludwig-Maximilians-Universität München, Theresienstraße 37, D-80333 München, Germany

⁴*Munich Center for Quantum Science and Technology (MCQST), Schellingstraße 4, D-80799 München, Germany*

⁵*Dahlem Center for Complex Quantum Systems,
Freie Universität Berlin, 14195 Berlin, Germany*

(Dated: March 29, 2024)

Quantum many-body scarring (QMBS) has emerged as an intriguing paradigm of weak ergodicity breaking in nonintegrable quantum many-body models, particularly lattice gauge theories (LGTs) in 1 + 1 spacetime dimensions. However, an open question is whether QMBS exists in higher-dimensional LGTs with dynamical matter. Given that nonergodic dynamics in $d=1$ spatial dimension tend to vanish in $d>1$, it is important to probe this question. Using matrix product state techniques for both finite and infinite systems, we show that QMBS occurs in the 2+1D U(1) quantum link model (QLM), as evidenced in persistent coherent oscillations in local observables, a marked slowdown in the growth of the bipartite entanglement entropy, and revivals in the fidelity. Interestingly, we see that QMBS is more robust when the matter degrees of freedom are bosonic rather than fermionic. Our results further shed light on the intimate connection between gauge invariance and QMBS, and highlight the persistence of scarring in higher spatial dimensions. Our findings can be tested in near-term analog and digital quantum simulators, and we demonstrate their accessibility on a recently proposed cold-atom analog quantum simulator.

Introduction.—QMBS is an exciting paradigm of ergodicity breaking in isolated quantum many-body models that are expected to thermalize [1–7]. Despite being ergodic, certain models host special nonthermal *scar* eigenstates that are roughly equally spaced in energy over the whole spectrum [8, 9], and exhibit anomalously low bipartite entanglement entropy [10, 11]. Upon preparing an initial state with a high overlap with these scar eigenstates, the system avoids thermalization and its dynamics exhibits long-lived coherent oscillations lasting well beyond all relevant timescales, with the time-evolved wave function undergoing persistent periodic revivals [8, 12]. QMBS is of great importance in investigations of the Eigenstate Thermalization Hypothesis (ETH) [13–16], as it facilitates violations of the latter through novel mechanisms based on spectrum-generating algebras [17–20] and nonthermal-eigenstate embedding [21]. QMBS has also been the subject of various experiments in both analog and digital quantum simulators [1, 22–26].

QMBS also has an intimate connection to lattice gauge theories (LGTs) [27–33], which are interacting quantum many-body models hosting gauge symmetries that enforce an intrinsic relation between the local distribution of matter and the allowed corresponding configurations of the gauge fields [34, 35]. Indeed, the quantum Ising-like model realized in a Rydberg setup that produced the first instance of QMBS [1] can be effectively described by the PXP model, which Surace *et al.* [27] have shown to map exactly onto the 1+1D spin-1/2 U(1) QLM [36, 37]. The spin-1/2 U(1) QLM is a formulation of the Schwinger model in which the gauge and electric fields are represented by spin-1/2 operators. This trun-

cation has facilitated experimental feasibility in the realization of large-scale quantum simulators of the spin-1/2 U(1) QLM [24, 38–40], with proposed algorithms for digital platforms [41], while still capturing salient features of the Schwinger model such as Coleman’s phase transition [42]. Given the ongoing strong drive of realizing quantum simulators of LGTs [43–53], it is important to fully understand the connection between QMBS and LGTs both from a fundamental point of view and also to facilitate experimental investigations.

In particular, it is interesting to see how QMBS behaves in 2+1D LGTs. Indeed, it is known that nonergodic features in 1+1D interacting models tend to vanish in higher spatial dimensions $d>1$, with many-body localization [54–57] being a prime example. How the *weak* ergodicity-breaking mechanism of QMBS fares for $d=2$ is a question that has recently received some attention in the context of the PXP model [58, 59] and helix states in the XXZ model [4], in addition to other quasi-2+1D systems [25, 26]. Nevertheless, scarred models in $d>1$ are far and few in between compared to their counterparts in $d=1$ [5–7]. This further motivates adding to the collection of such models by investigating LGTs with dynamical matter in higher spatial dimensions.

Indeed, QMBS in LGTs in $d>1$ has been studied [30, 60, 61], but only in the case without dynamical matter, where connections to high-energy phenomena are not as straightforward. In trying to see whether QMBS will persist in the quantum-field-theory limit of gauge theories, such as in quantum electrodynamics, the inclusion of dynamical matter is important [31, 32].

In this Letter, we consider the 2+1D spin-1/2 U(1)

QLM with dynamical matter on a square lattice, and show that QMBS persists for special far-from-equilibrium quenches. We also showcase how these QMBS regimes can be detected in near-term analog quantum simulators of LGTs in $d=2$ spatial dimensions.

Model.—We consider the U(1) QLM on a square lattice described by the Hamiltonian [36, 37]

$$\hat{H} = \sum_{\mathbf{r}} \left[-\frac{\kappa}{2} \left(\hat{\phi}_{\mathbf{r}}^{\dagger} \hat{s}_{\mathbf{r},\mathbf{e}_x}^{+} \hat{\phi}_{\mathbf{r}+\mathbf{e}_x} + \alpha (-1)^{r_y} \hat{\phi}_{\mathbf{r}}^{\dagger} \hat{s}_{\mathbf{r},\mathbf{e}_y}^{+} \hat{\phi}_{\mathbf{r}+\mathbf{e}_y} + \text{H.c.} \right) + m (-1)^{r_x+r_y} \hat{\phi}_{\mathbf{r}}^{\dagger} \hat{\phi}_{\mathbf{r}} - \alpha^2 J \left(\hat{U}_{\square_{\mathbf{r}}} + \hat{U}_{\square_{\mathbf{r}}}^{\dagger} \right) \right]. \quad (1)$$

The matter degrees of freedom with mass m are represented by the ladder operators $\hat{\phi}_{\mathbf{r}}^{(\dagger)}$ at site \mathbf{r} . These can either be fermionic or hard-core bosonic, and we will consider both in this Letter. The gauge (electric) field is represented by the spin-1/2 operator $\hat{s}_{\mathbf{r},\mathbf{e}_a}^{+(z)}$, where the subscript denotes the bond between sites \mathbf{r} and $\mathbf{r}+\mathbf{e}_a$, where \mathbf{e}_a is a unit vector ($a=x,y$). The magnetic interactions of the gauge fields, whose strength is proportional to J , are represented by the plaquette operators $\hat{U}_{\square_{\mathbf{r}}} = \hat{s}_{\mathbf{r},\mathbf{e}_x}^{+} \hat{s}_{\mathbf{r}+\mathbf{e}_x,\mathbf{e}_y}^{+} \hat{s}_{\mathbf{r}+\mathbf{e}_y,\mathbf{e}_x}^{-} \hat{s}_{\mathbf{r},\mathbf{e}_y}^{-}$. The coefficient α is used to tune the ratio of the coupling along the y and x axes, such that the couplings are equally strong at $\alpha = 1$, and at $\alpha = 0$, only the coupling along the x axis remains, and the system behaves like a collection of uncoupled 1 + 1D QLMs. Thus, by using $0 < \alpha < 1$, we can interpolate between the 2 + 1D square lattice ($\alpha = 1$) and the 1 + 1D model ($\alpha = 0$).

The U(1) gauge symmetry of this model is generated by the operators

$$\hat{G}_{\mathbf{r}} = \hat{\phi}_{\mathbf{r}}^{\dagger} \hat{\phi}_{\mathbf{r}} - \frac{1 - (-1)^{r_x+r_y}}{2} - \sum_{a=x,y} [\hat{s}_{\mathbf{r},\mathbf{e}_a}^z - \hat{s}_{\mathbf{r}-\mathbf{e}_a,\mathbf{e}_a}^z], \quad (2)$$

which act as a discrete analog of Gauss's law. We work in the physical sector of states, which are eigenstates of $\hat{G}_{\mathbf{r}}$ for each \mathbf{r} with eigenvalue zero. Given a configuration of the matter sites, this becomes a constraint on the allowed configuration on the gauge sites: the allowed configurations surrounding occupied and unoccupied matter sites are shown in Fig. 1(a).

Scarring dynamics.—Here we consider the dynamics following the global quench of an initial charge-proliferated state $|\psi(t=0)\rangle$, being the gauge-invariant ground state at $m/\kappa \rightarrow -\infty$, using the gauge site configuration shown in Fig. 1(b) (which is chosen such that at $\alpha = 0$, the decoupled chains are in the physical gauge sector of the 1+1D model). We quench to a finite value of the mass m , which is known to lead to scarred dynamics in the 1+1D model [24, 62, 63], in particular, we quench to $m = 0.84\kappa$, which is the regime considered in the experiment of Ref. [24], while setting $J = 0$. We use numerical time-evolution simulations to obtain these dynamics based on matrix product state (MPS) techniques [64–66].

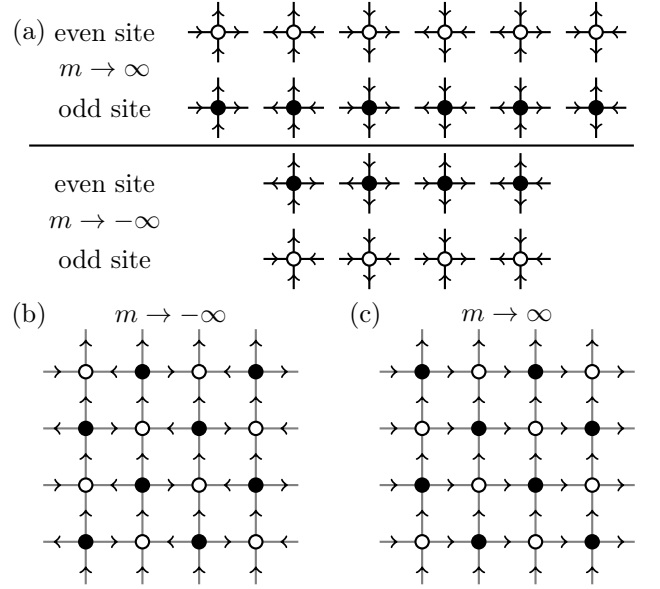


FIG. 1. (a) The gauge-invariant configurations for the gauge sites surrounding each matter site in the spin-1/2 U(1) quantum link model (1), according to Gauss's law (2). The site parity refers to the parity of the sum of the x and y components of the index: $r_x + r_y$. Arrows pointing right or up on gauge sites represent eigenstates of \hat{s}^z with eigenvalue $+1/2$, while arrows pointing left or down represent the eigenvalue $-1/2$. (b) A charge-proliferated ground state at $m \rightarrow -\infty$. (c) A vacuum ground state at $m \rightarrow \infty$.

Specifically, we use the time-dependent variational principle (TDVP) algorithm [67], using single-site updates with adaptive bond dimension expansion. Simulations were performed using a cylindrical lattice geometry, with a circumference of $L_y = 4$ matter sites: we perform calculations using states which are explicitly translation invariant along the x -axis, as well as states with a finite length $L_x = 16$ in order to calculate the fidelity with the initial state, using open boundaries at the ends of the cylinder.

The quench simulation results are displayed in Figures 2 and 3, for bosonic and fermionic matter statistics respectively, as the coupling ratio α is tuned from one to zero. In panels (a), we show the expectation value of the chiral condensate $\mathcal{C}(t) = \langle \psi(t) | \hat{\mathcal{C}} | \psi(t) \rangle$,

$$\hat{\mathcal{C}} = \frac{1}{L_x L_y} \sum_{\mathbf{r}} (-1)^{r_x+r_y} \left(\hat{\phi}_{\mathbf{r}}^{\dagger} \hat{\phi}_{\mathbf{r}} - \frac{1 - (-1)^{r_x+r_y}}{2} \right), \quad (3)$$

in panels (b), we show the von Neumann entanglement entropy $\mathcal{S}(t)$ measured using a bipartition formed by a slice along the circumference of the cylinder, and in panels (c), we show the fidelity with the initial state $\mathcal{F}(t) = |\langle \psi(0) | \psi(t) \rangle|^2$ for the finite system.

For the quenches with bosonic matter (Fig. 2), we can see the signatures of QMBS are qualitatively preserved, although less pronounced, as α increases from

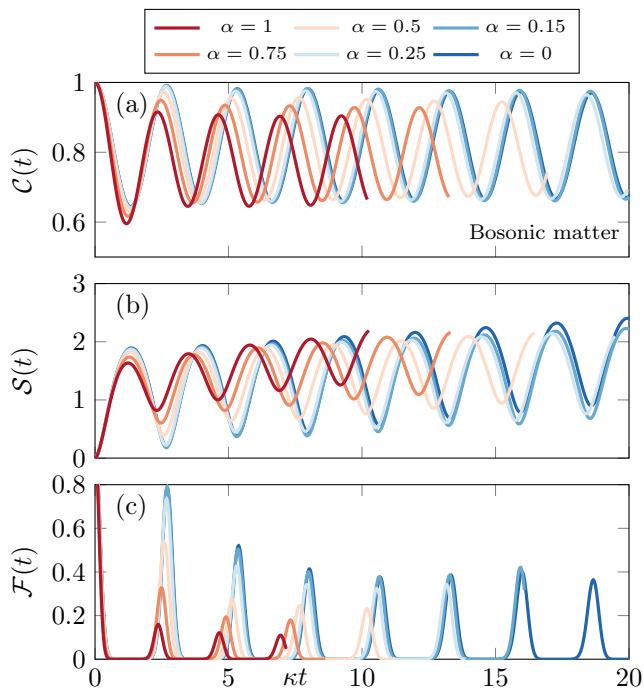


FIG. 2. A numerical time-evolution simulation of the quench of the charge-proliferated state shown in Fig. 1(b) to $m = 0.84\kappa$, using matter with bosonic statistics on a $L_y = 4$ cylinder, as the coupling ratio α tuned from 1 to 0. (a) The chiral condensate $\mathcal{C}(t)$ (3) and (b) entanglement entropy across a circumferential slice $\mathcal{S}(t)$, calculated for an infinite-length cylinder. (c) The fidelity $\mathcal{F}(t)$, calculated for a finite cylinder of dimension 4×16 with open boundaries in the x direction.

zero (where the dynamics will correspond to the 1 + 1D QLM) up to one (where we retrieve the fully fledged 2 + 1D QLM). The oscillatory behavior of the chiral condensate (Fig. 2(a)) and entanglement entropy (Fig. 2(b)) is clearly visible for all values of α throughout the whole simulation, and the fidelity (Fig. 2(c)) shows revivals of a consistent, though weaker, magnitude. However, in the fermionic matter quenches (Fig. 3), the signatures of QMBS clearly break down as α is increased. The oscillations in the chiral condensate (Fig. 3(a)) quickly decay in magnitude, the growth of the entanglement entropy (Fig. 3(b)) is significantly more rapid, and the revivals in fidelity (Fig. 3(c)) also swiftly decrease in magnitude. These results show that the fate of QMBS in the 2 + 1D QLM is strongly dependent on the particle statistics of the matter degrees of freedom, as the signs of scarring are preserved for bosonic, but not fermionic, matter. Nevertheless, it is quite an interesting finding to see that QMBS persists and is rather robust in $d = 2$ spatial dimensions in the presence of hard-core bosonic dynamical matter.

We also find that the plaquette term weakens the QMBS observed in Figs. 2 and 3, with more suppressed QMBS the larger J is; see Supplemental Material (SM) [68]. We have also investigated quenching from the vac-

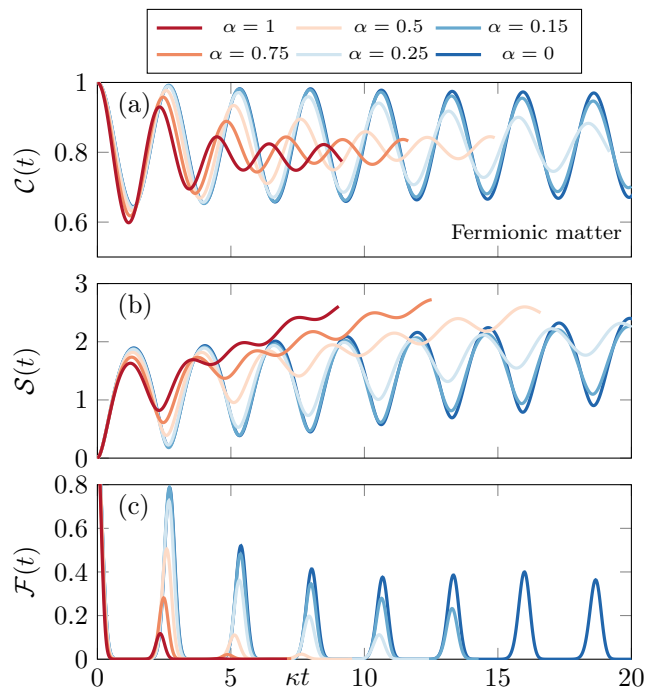


FIG. 3. A numerical time-evolution simulation of the quench of the charge-proliferated state shown in Fig. 1(b) to $m = 0.84\kappa$, using matter with fermionic statistics on a $L_y = 4$ cylinder, as the coupling ratio α tuned from 1 to 0. (a) The chiral condensate $\mathcal{C}(t)$ (3) and (b) entanglement entropy across a circumferential slice $\mathcal{S}(t)$, calculated for an infinite-length cylinder. (c) The fidelity $\mathcal{F}(t)$, calculated for a finite cylinder of dimension 4×16 with open boundaries in the x direction.

uum states of the 2 + 1D QLM, but we have found no signs of QMBS regardless of whether the matter degrees of freedom are fermionic or hard-core bosonic [68].

Quantum simulation.—In order to demonstrate the relevance of these results to near-term quantum simulators, we show that the dynamics for the bosonic QLM (Fig. 2) can be probed using the 2D Bose–Hubbard simulator proposed in Ref. [69] (see Fig. 4(a) for the mapping of the charge-proliferated state), with the Hamiltonian

$$\hat{H}_{\text{BHM}} = \sum_{\mathbf{j}} \left[\tilde{\mathbf{j}} \sum_{a=x,y} \left(\hat{b}_{\mathbf{j}}^\dagger \hat{b}_{\mathbf{j}+\mathbf{e}_a} + \text{H.c.} \right) + \frac{U_{\mathbf{j}}}{2} \hat{n}_{\mathbf{j}} (\hat{n}_{\mathbf{j}} - 1) + (\tilde{\gamma} \cdot \mathbf{j} - \delta_{\mathbf{j}} - \eta_{\mathbf{j}}) \hat{n}_{\mathbf{j}} \right]. \quad (4)$$

Here, the lattice site of index $\mathbf{j} = (j_x, j_y)$ corresponds to a matter site in the QLM if both components are even, to a gauge site if exactly one of them is even, or if both components are odd the site is forbidden from contributing to the dynamics. $\hat{b}_{\mathbf{j}}^{(\dagger)}$ and $\hat{n}_{\mathbf{j}} = \hat{b}_{\mathbf{j}}^\dagger \hat{b}_{\mathbf{j}}$ are the bosonic ladder and number operators respectively, the on-site interaction strength $U_{\mathbf{j}}$ is equal to U on gauge and forbidden sites, but $\tilde{\alpha}U$ on matter sites, for some detuning constant $\tilde{\alpha}$, $\tilde{\gamma} = (\gamma_x, \gamma_y)$ represents a linear tilt in the lattice

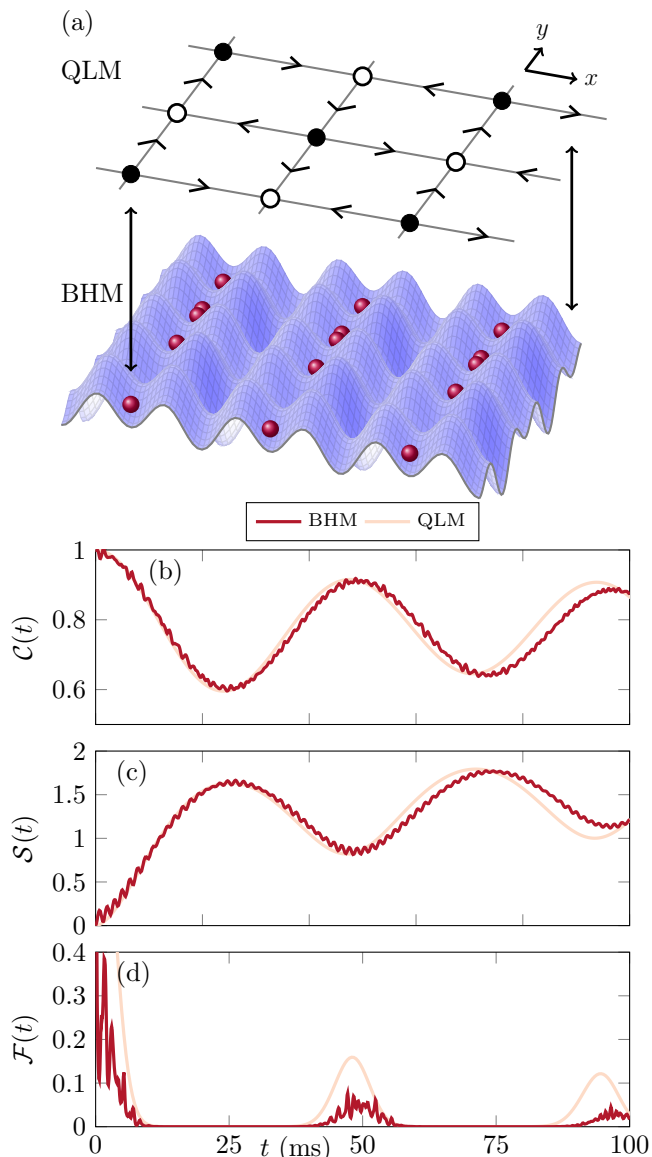


FIG. 4. (a) The mapping between the 2 + 1D U(1) QLM and the Bose-Hubbard simulator proposed in Ref. [69]. (b-d) A numerical time-evolution simulation of the quench of the charge-proliferated state shown in (a) to $m = 0.84\kappa$ on a $L_y = 4$ cylinder for Bose-Hubbard simulator (4), compared with the QLM simulation in Fig. 2, showing the chiral condensate $C(t)$ (3), entanglement entropy $S(t)$, and fidelity with the initial state $F(t)$.

in both dimensions, and the potential δ_j (η_j) is equal to δ (η) only on a gauge (forbidden) site, and zero elsewhere. Following Ref. [69], we use the values of the parameters $\tilde{J} = 30$ Hz, $U = 1300$ Hz, $\tilde{\alpha} = 1.3$, $\gamma_x = 57$ Hz, $\gamma_y = 73$ Hz, $\delta = 649.647$ Hz, and $\eta = 5\delta$. This corresponds to $m \approx -0.84\kappa$ in the QLM (quenches starting from the charge-proliferated initial state Fig. 1(b) have the same dynamics for positive and negative m). The results of the quench of the charge-proliferated initial state

in Fig. 4(a) are shown in Fig. 4(b-d), compared with the QLM simulation (Fig. 2) using the simulator's effective value of κ , which show great agreement for the available simulation times. This bodes well for upcoming cold-atom experiments seeking to realize 2 + 1D U(1) QLMs, as it brings our findings into the realm of experimental accessibility.

Discussion and outlook.—We have studied QMBS in a spin-1/2 2 + 1D U(1) QLM with dynamical matter using MPS simulations of quench dynamics. We have found that QMBS is robust when the initial state is the charge-proliferated product state and the quench mass is $m \approx 0.84\kappa$, particularly when the matter degrees of freedom are hard-core bosonic. In the case of fermionic matter, we have found that scarring persists only for short times, but then vanishes and the dynamics looks quite ergodic. We have also adopted in our simulations a ratio α between coupling in the x and y directions. When $\alpha = 0$, we are effectively in 1 + 1D, and so we can retrieve the established QMBS regimes there. Upon tuning α up to unity (the fully fledged 2 + 1D system), we see that scarring unsurprisingly gets weaker, but does not always vanish, as explained above. In this work we have used $4 \times \infty$ and 4×16 cylinders, but we expect that the same qualitative picture remains for wider cylinders [70, 71].

We have also showcased how our findings can be tested on a recently proposed cold-atom quantum simulator of the spin-1/2 U(1) QLM with hard-core bosonic matter degrees of freedom [69], showing great agreement between the simulator dynamics and those of the ideal QLM. But our results are also amenable for investigation in other proposals that have been put forth [72–75]. Given that going to $d = 2$ spatial dimensions in quantum-simulator realizations of LGTs is the current frontier of the field [48], our work sets the stage for experimentally relevant features that can be probed on such devices once they are available.

It is important to emphasize that our work does not rule out other QMBS regimes that may still persist in 2 + 1D but that we have not found. Indeed, our goal in this work was to investigate the fate of QMBS regimes discovered in the 1 + 1D U(1) QLM and see how well they fare in 2 + 1D. It was also our intention to find out how the statistics of the matter degrees of freedom affects QMBS, which, as we show, happens in a profound way. One avenue for future work is to study the fate of the QMBS regime we find in 2 + 1D for higher-level representations ($S > 1/2$) of the electric and gauge fields. In 1 + 1D, it has been shown that scarring persists and is robust for $S > 1/2$ [31, 32]. This is important to assess the fate of QMBS in the limit of 2 + 1D lattice QED, and a recent proposal may allow experimental observation in a quantum simulator of the spin-1 U(1) QLM [76]. A second venue involves adding a topological θ -term [77, 78] and studying its interplay with scarring in 2 + 1D, which has been shown to lead to a plethora of nonergodic

behavior is $1 + 1D$ [79].

Note.—During the final stages of preparing our manuscript, we became aware of another work [80] on quantum many-body scars for arbitrary integer spin in $2 + 1D$ pure Abelian gauge theories. This work will appear in the same arXiv listing as ours.

Acknowledgments.—The authors are grateful to Jean-Yves Desaulles and Zlatko Papić for fruitful discussions. This work is supported by the Emmy Noether Programme of the German Research Foundation (DFG) under grant no. HA 8206/1-1. I.P.M. acknowledges funding from the National Science and Technology Council (NSTC) Grant No. 122-2811-M-007-044. Numerical simulations were performed on The University of Queensland’s School of Mathematics and Physics Core Computing Facility getafix.

* jad.halimeh@physik.lmu.de

- [1] Hannes Bernien, Sylvain Schwartz, Alexander Keesling, Harry Levine, Ahmed Omran, Hannes Pichler, Soonwon Choi, Alexander S. Zibrov, Manuel Endres, Markus Greiner, Vladan Vuletić, and Mikhail D. Lukin, “Probing many-body dynamics on a 51-atom quantum simulator,” *Nature* **551**, 579–584 (2017).
- [2] Sanjay Moudgalya, Stephan Rachel, B. Andrei Bernevig, and Nicolas Regnault, “Exact excited states of nonintegrable models,” *Phys. Rev. B* **98**, 235155 (2018).
- [3] Hongzheng Zhao, Joseph Vovrosh, Florian Mintert, and Johannes Knolle, “Quantum many-body scars in optical lattices,” *Phys. Rev. Lett.* **124**, 160604 (2020).
- [4] Paul Niklas Jepsen, Yoo Kyung ‘Eunice’ Lee, Hanzhen Lin, Ivana Dimitrova, Yair Margalit, Wen Wei Ho, and Wolfgang Ketterle, “Long-lived phantom helix states in heisenberg quantum magnets,” *Nature Physics* **18**, 899–904 (2022).
- [5] Maksym Serbyn, Dmitry A. Abanin, and Zlatko Papić, “Quantum many-body scars and weak breaking of ergodicity,” *Nature Physics* **17**, 675–685 (2021).
- [6] Sanjay Moudgalya, B Andrei Bernevig, and Nicolas Regnault, “Quantum many-body scars and hilbert space fragmentation: a review of exact results,” *Reports on Progress in Physics* **85**, 086501 (2022).
- [7] Anushya Chandran, Thomas Iadecola, Vedika Khemani, and Roderich Moessner, “Quantum many-body scars: A quasiparticle perspective,” *Annual Review of Condensed Matter Physics* **14**, 443–469 (2023), <https://doi.org/10.1146/annurev-conmatphys-031620-101617>.
- [8] C. J. Turner, A. A. Michailidis, D. A. Abanin, M. Serbyn, and Z. Papić, “Weak ergodicity breaking from quantum many-body scars,” *Nature Physics* **14**, 745–749 (2018).
- [9] Michael Schecter and Thomas Iadecola, “Weak ergodicity breaking and quantum many-body scars in spin-1 xy magnets,” *Phys. Rev. Lett.* **123**, 147201 (2019).
- [10] Sanjay Moudgalya, Nicolas Regnault, and B. Andrei Bernevig, “Entanglement of exact excited states of Affleck-Kennedy-Lieb-Tasaki models: Exact results, many-body scars, and violation of the strong eigenstate thermalization hypothesis,” *Phys. Rev. B* **98**, 235156 (2018).
- [11] Cheng-Ju Lin and Olexei I. Motrunich, “Exact quantum many-body scar states in the Rydberg-blockaded atom chain,” *Phys. Rev. Lett.* **122**, 173401 (2019).
- [12] Wen Wei Ho, Soonwon Choi, Hannes Pichler, and Mikhail D. Lukin, “Periodic orbits, entanglement, and quantum many-body scars in constrained models: Matrix product state approach,” *Phys. Rev. Lett.* **122**, 040603 (2019).
- [13] J. M. Deutsch, “Quantum statistical mechanics in a closed system,” *Phys. Rev. A* **43**, 2046–2049 (1991).
- [14] Mark Srednicki, “Chaos and quantum thermalization,” *Phys. Rev. E* **50**, 888–901 (1994).
- [15] Luca D’Alessio, Yariv Kafri, Anatoli Polkovnikov, and Marcos Rigol, “From quantum chaos and eigenstate thermalization to statistical mechanics and thermodynamics,” *Advances in Physics* **65**, 239–362 (2016).
- [16] Joshua M Deutsch, “Eigenstate thermalization hypothesis,” *Reports on Progress in Physics* **81**, 082001 (2018).
- [17] Daniel K. Mark, Cheng-Ju Lin, and Olexei I. Motrunich, “Unified structure for exact towers of scar states in the Affleck-Kennedy-Lieb-Tasaki and other models,” *Phys. Rev. B* **101**, 195131 (2020).
- [18] Sanjay Moudgalya, Nicolas Regnault, and B. Andrei Bernevig, “ η -pairing in Hubbard models: From spectrum generating algebras to quantum many-body scars,” *Phys. Rev. B* **102**, 085140 (2020).
- [19] Nicholas O’Dea, Fiona Burnell, Anushya Chandran, and Vedika Khemani, “From tunnels to towers: Quantum scars from Lie algebras and q -deformed Lie algebras,” *Phys. Rev. Research* **2**, 043305 (2020).
- [20] K. Pakrouski, P. N. Pallegar, F. K. Popov, and I. R. Klebanov, “Many-body scars as a group invariant sector of Hilbert space,” *Phys. Rev. Lett.* **125**, 230602 (2020).
- [21] Naoto Shiraishi and Takashi Mori, “Systematic construction of counterexamples to the eigenstate thermalization hypothesis,” *Phys. Rev. Lett.* **119**, 030601 (2017).
- [22] D. Bluvstein, A. Omran, H. Levine, A. Keesling, G. Semeghini, S. Ebadi, T. T. Wang, A. A. Michailidis, N. Maskara, W. W. Ho, S. Choi, M. Serbyn, M. Greiner, V. Vuletić, and M. D. Lukin, “Controlling quantum many-body dynamics in driven Rydberg atom arrays,” *Science* **371**, 1355–1359 (2021).
- [23] Dolev Bluvstein, Harry Levine, Giulia Semeghini, Tout T. Wang, Sepehr Ebadi, Marcin Kalinowski, Alexander Keesling, Nishad Maskara, Hannes Pichler, Markus Greiner, Vladan Vuletić, and Mikhail D. Lukin, “A quantum processor based on coherent transport of entangled atom arrays,” *Nature* **604**, 451–456 (2022).
- [24] Guo-Xian Su, Hui Sun, Ana Hudomal, Jean-Yves Desaulles, Zhao-Yu Zhou, Bing Yang, Jad C. Halimeh, Zhen-Sheng Yuan, Zlatko Papić, and Jian-Wei Pan, “Observation of many-body scarring in a bose-hubbard quantum simulator,” *Phys. Rev. Res.* **5**, 023010 (2023).
- [25] Pengfei Zhang, Hang Dong, Yu Gao, Liangtian Zhao, Jie Hao, Jean-Yves Desaulles, Qiujiang Guo, Jiachen Chen, Jinfeng Deng, Bobo Liu, Wenhui Ren, Yunyan Yao, Xu Zhang, Shibo Xu, Ke Wang, Feitong Jin, Xuhao Zhu, Bing Zhang, Hekang Li, Chao Song, Zhen Wang, Fangli Liu, Zlatko Papić, Lei Ying, H. Wang, and Ying-Cheng Lai, “Many-body hilbert space scarring on a superconducting processor,” *Nature Physics* **19**, 120–125 (2023).
- [26] Hang Dong, Jean-Yves Desaulles, Yu Gao, Ning Wang,

- Zexian Guo, Jiachen Chen, Yiren Zou, Feitong Jin, Xuhao Zhu, Pengfei Zhang, Hekang Li, Zhen Wang, Qiujiang Guo, Junxiang Zhang, Lei Ying, and Zlatko Papić, “Disorder-tunable entanglement at infinite temperature,” *Science Advances* **9**, eadj3822 (2023), <https://www.science.org/doi/pdf/10.1126/sciadv.adj3822>.
- [27] Federica M. Surace, Paolo P. Mazza, Giuliano Giudici, Alessio Lerose, Andrea Gambassi, and Marcello Dalmonte, “Lattice gauge theories and string dynamics in Rydberg atom quantum simulators,” *Phys. Rev. X* **10**, 021041 (2020).
- [28] Thomas Iadecola and Michael Schecter, “Quantum many-body scar states with emergent kinetic constraints and finite-entanglement revivals,” *Phys. Rev. B* **101**, 024306 (2020).
- [29] Adith Sai Aramthottil, Utso Bhattacharya, Daniel González-Cuadra, Maciej Lewenstein, Luca Barbiero, and Jakub Zakrzewski, “Scar states in deconfined z_2 lattice gauge theories,” *Phys. Rev. B* **106**, L041101 (2022).
- [30] Saptarshi Biswas, Debasish Banerjee, and Arnab Sen, “Scars from protected zero modes and beyond in $U(1)$ quantum link and quantum dimer models,” *SciPost Phys.* **12**, 148 (2022).
- [31] Jean-Yves Desaulles, Debasish Banerjee, Ana Hudomal, Zlatko Papić, Arnab Sen, and Jad C. Halimeh, “Weak ergodicity breaking in the schwinger model,” *Phys. Rev. B* **107**, L201105 (2023).
- [32] Jean-Yves Desaulles, Ana Hudomal, Debasish Banerjee, Arnab Sen, Zlatko Papić, and Jad C. Halimeh, “Prominent quantum many-body scars in a truncated schwinger model,” *Phys. Rev. B* **107**, 205112 (2023).
- [33] Jad C. Halimeh, Luca Barbiero, Philipp Hauke, Fabian Grusdt, and Annabelle Bohrdt, “Robust quantum many-body scars in lattice gauge theories,” *Quantum* **7**, 1004 (2023).
- [34] S. Weinberg, *The Quantum Theory of Fields*, Vol. 2: Modern Applications (Cambridge University Press, 1995).
- [35] M. E. Peskin and D. V. Schroeder, *An Introduction To Quantum Field Theory* (CRC Press, 2018).
- [36] S Chandrasekharan and U.-J Wiese, “Quantum link models: A discrete approach to gauge theories,” *Nuclear Physics B* **492**, 455 – 471 (1997).
- [37] U.-J. Wiese, “Ultracold quantum gases and lattice systems: quantum simulation of lattice gauge theories,” *Annalen der Physik* **525**, 777–796 (2013).
- [38] Bing Yang, Hui Sun, Robert Ott, Han-Yi Wang, Torsten V. Zache, Jad C. Halimeh, Zhen-Sheng Yuan, Philipp Hauke, and Jian-Wei Pan, “Observation of gauge invariance in a 71-site Bose–Hubbard quantum simulator,” *Nature* **587**, 392–396 (2020).
- [39] Zhao-Yu Zhou, Guo-Xian Su, Jad C. Halimeh, Robert Ott, Hui Sun, Philipp Hauke, Bing Yang, Zhen-Sheng Yuan, Jürgen Berges, and Jian-Wei Pan, “Thermalization dynamics of a gauge theory on a quantum simulator,” *Science* **377**, 311–314 (2022).
- [40] Wei-Yong Zhang, Ying Liu, Yanting Cheng, Ming-Gen He, Han-Yi Wang, Tian-Yi Wang, Zi-Hang Zhu, Guo-Xian Su, Zhao-Yu Zhou, Yong-Guang Zheng, Hui Sun, Bing Yang, Philipp Hauke, Wei Zheng, Jad C. Halimeh, Zhen-Sheng Yuan, and Jian-Wei Pan, “Observation of microscopic confinement dynamics by a tunable topological θ -angle,” (2023), [arXiv:2306.11794 \[cond-mat.quant-gas\]](https://arxiv.org/abs/2306.11794).
- [41] Joao C. Pinto Barros, Thea Budde, and Marina Krstic Marinkovic, “Meron-cluster algorithms for quantum link models,” (2024), [arXiv:2402.01039 \[hep-lat\]](https://arxiv.org/abs/2402.01039).
- [42] Sidney Coleman, “More about the massive schwinger model,” *Annals of Physics* **101**, 239 – 267 (1976).
- [43] M. Dalmonte and S. Montangero, “Lattice gauge theory simulations in the quantum information era,” *Contemporary Physics* **57**, 388–412 (2016).
- [44] Mari Carmen Bañuls, Rainer Blatt, Jacopo Catani, Alessio Celi, Juan Ignacio Cirac, Marcello Dalmonte, Leonardo Fallani, Karl Jansen, Maciej Lewenstein, Simone Montangero, Christine A. Muschik, Benni Reznik, Enrique Rico, Luca Tagliacozzo, Karel Van Acoleyen, Frank Verstraete, Uwe-Jens Wiese, Matthew Wingate, Jakub Zakrzewski, and Peter Zoller, “Simulating lattice gauge theories within quantum technologies,” *The European Physical Journal D* **74**, 165 (2020).
- [45] Erez Zohar, J Ignacio Cirac, and Benni Reznik, “Quantum simulations of lattice gauge theories using ultracold atoms in optical lattices,” *Reports on Progress in Physics* **79**, 014401 (2015).
- [46] Yuri Alexeev, Dave Bacon, Kenneth R. Brown, Robert Calderbank, Lincoln D. Carr, Frederic T. Chong, Brian DeMarco, Dirk Englund, Edward Farhi, Bill Fefferman, Alexey V. Gorshkov, Andrew Houck, Jungsang Kim, Shelby Kimmel, Michael Lange, Seth Lloyd, Mikhail D. Lukin, Dmitri Maslov, Peter Maunz, Christopher Monroe, John Preskill, Martin Roetteler, Martin J. Savage, and Jeff Thompson, “Quantum computer systems for scientific discovery,” *PRX Quantum* **2**, 017001 (2021).
- [47] Monika Aidelsburger, Luca Barbiero, Alejandro Bermudez, Titas Chanda, Alexandre Dauphin, Daniel González-Cuadra, Przemysław R. Grzybowski, Simon Hands, Fred Jendrzejewski, Johannes Jünemann, Gediminas Juzeliūnas, Valentin Kasper, Angelo Piga, Shi-Ju Ran, Matteo Rizzi, Germán Sierra, Luca Tagliacozzo, Emanuele Tirrito, Torsten V. Zache, Jakub Zakrzewski, Erez Zohar, and Maciej Lewenstein, “Cold atoms meet lattice gauge theory,” *Philosophical Transactions of the Royal Society A: Mathematical, Physical and Engineering Sciences* **380**, 20210064 (2022).
- [48] Erez Zohar, “Quantum simulation of lattice gauge theories in more than one space dimension—requirements, challenges and methods,” *Philosophical Transactions of the Royal Society of London Series A* **380**, 20210069 (2022), [arXiv:2106.04609 \[quant-ph\]](https://arxiv.org/abs/2106.04609).
- [49] Natalie Kleo, Alessandro Roggero, and Martin J. Savage, “Standard model physics and the digital quantum revolution: Thoughts about the interface,” *arXiv preprint* (2021), [arXiv:2107.04769 \[quant-ph\]](https://arxiv.org/abs/2107.04769).
- [50] Christian W. Bauer, Zohreh Davoudi, A. Baha Balantekin, Tanmoy Bhattacharya, Marcela Carena, Wibe A. de Jong, Patrick Draper, Aida El-Khadra, Nate Gemelke, Masanori Hanada, Dmitri Kharzeev, Henry Lamm, Ying-Ying Li, Junyu Liu, Mikhail Lukin, Yannick Meurice, Christopher Monroe, Benjamin Nachman, Guido Pagano, John Preskill, Enrico Rinaldi, Alessandro Roggero, David I. Santiago, Martin J. Savage, Ifan Siddiqi, George Siopsis, David Van Zanten, Nathan Wiebe, Yukari Yamauchi, Kübra Yeter-Aydeniz, and Silvia Zorzetti, “Quantum simulation for high-energy physics,” *PRX Quantum* **4**, 027001 (2023).
- [51] Alberto Di Meglio, Karl Jansen, Ivano Tavernelli, Constantia Alexandrou, Srinivasan Arunachalam, Chris-

- tian W. Bauer, Kerstin Borrás, Stefano Carrazza, Arianna Crippa, Vincent Croft, Roland de Putter, Andrea Delgado, Vedran Dunjko, Daniel J. Egger, Elias Fernandez-Combarro, Elina Fuchs, Lena Funcke, Daniel Gonzalez-Cuadra, Michele Grossi, Jad C. Halimeh, Zoe Holmes, Stefan Kuhn, Denis Lacroix, Randy Lewis, Donatella Lucchesi, Miriam Lucio Martinez, Federico Meloni, Antonio Mezzacapo, Simone Montangero, Lento Nagano, Voica Radescu, Enrique Rico Ortega, Alessandro Roggero, Julian Schuhmacher, Joao Seixas, Pietro Silvi, Panagiotis Spentzouris, Francesco Tacchino, Kristan Temme, Koji Terashi, Jordi Tura, Cenk Tuysuz, Sofia Vallecorsa, Uwe-Jens Wiese, Shinjae Yoo, and Jinglei Zhang, “Quantum computing for high-energy physics: State of the art and challenges. summary of the qc4hep working group,” (2023), [arXiv:2307.03236 \[quant-ph\]](https://arxiv.org/abs/2307.03236).
- [52] Jad C. Halimeh, Monika Aidelsburger, Fabian Grusdt, Philipp Hauke, and Bing Yang, “Cold-atom quantum simulators of gauge theories,” (2023), [arXiv:2310.12201 \[cond-mat.quant-gas\]](https://arxiv.org/abs/2310.12201).
- [53] Yanting Cheng and Hui Zhai, “Emergent gauge theory in rydberg atom arrays,” (2024), [arXiv:2401.07708 \[cond-mat.quant-gas\]](https://arxiv.org/abs/2401.07708).
- [54] D.M. Basko, I.L. Aleiner, and B.L. Altshuler, “Metal-insulator transition in a weakly interacting many-electron system with localized single-particle states,” *Annals of Physics* **321**, 1126–1205 (2006).
- [55] I. V. Gornyi, A. D. Mirlin, and D. G. Polyakov, “Interacting electrons in disordered wires: Anderson localization and low- t transport,” *Phys. Rev. Lett.* **95**, 206603 (2005).
- [56] Rahul Nandkishore and David A. Huse, “Many-body localization and thermalization in quantum statistical mechanics,” *Annual Review of Condensed Matter Physics* **6**, 15–38 (2015).
- [57] Dmitry A. Abanin, Ehud Altman, Immanuel Bloch, and Maksym Serbyn, “Colloquium: Many-body localization, thermalization, and entanglement,” *Rev. Mod. Phys.* **91**, 021001 (2019).
- [58] A. A. Michailidis, C. J. Turner, Z. Papić, D. A. Abanin, and M. Serbyn, “Stabilizing two-dimensional quantum scars by deformation and synchronization,” *Phys. Rev. Res.* **2**, 022065 (2020).
- [59] Cheng-Ju Lin, Vladimir Calvera, and Timothy H. Hsieh, “Quantum many-body scar states in two-dimensional rydberg atom arrays,” *Phys. Rev. B* **101**, 220304 (2020).
- [60] Debasish Banerjee and Arnab Sen, “Quantum scars from zero modes in an abelian lattice gauge theory on ladders,” *Phys. Rev. Lett.* **126**, 220601 (2021).
- [61] Indrajit Sau, Paolo Stornati, Debasish Banerjee, and Arnab Sen, “Sublattice scars and beyond in two-dimensional $u(1)$ quantum link lattice gauge theories,” *Phys. Rev. D* **109**, 034519 (2024).
- [62] Ana Hudomal, Jean-Yves Desaulles, Bhaskar Mukherjee, Guo-Xian Su, Jad C. Halimeh, and Zlatko Papić, “Driving quantum many-body scars in the pxp model,” *Phys. Rev. B* **106**, 104302 (2022).
- [63] Aiden Daniel, Andrew Hallam, Jean-Yves Desaulles, Ana Hudomal, Guo-Xian Su, Jad C. Halimeh, and Zlatko Papić, “Bridging quantum criticality via many-body scarring,” *Phys. Rev. B* **107**, 235108 (2023).
- [64] Ulrich Schollwöck, “The density-matrix renormalization group in the age of matrix product states,” *Annals of Physics* **326**, 96–192 (2011), january 2011 Special Issue.
- [65] Sebastian Paeckel, Thomas Köhler, Andreas Swoboda, Salvatore R. Manmana, Ulrich Schollwöck, and Claudius Hubig, “Time-evolution methods for matrix-product states,” *Annals of Physics* **411**, 167998 (2019).
- [66] Ian P. McCulloch and J. Osborne, “Matrix product toolkit,” <https://github.com/mptoolkit>.
- [67] Jutho Haegeman, Christian Lubich, Ivan Oseledets, Bart Vandereycken, and Frank Verstraete, “Unifying time evolution and optimization with matrix product states,” *Phys. Rev. B* **94**, 165116 (2016).
- [68] See Supplemental Material for supporting numerical results.
- [69] Jesse Osborne, Ian P. McCulloch, Bing Yang, Philipp Hauke, and Jad C. Halimeh, “Large-scale 2 + 1D $U(1)$ gauge theory with dynamical matter in a cold-atom quantum simulator,” (2022), [arXiv:2211.01380 \[cond-mat.quant-gas\]](https://arxiv.org/abs/2211.01380).
- [70] Tomohiro Hashizume, Ian P. McCulloch, and Jad C. Halimeh, “Dynamical phase transitions in the two-dimensional transverse-field ising model,” *Phys. Rev. Res.* **4**, 013250 (2022).
- [71] Tomohiro Hashizume, Jad C. Halimeh, Philipp Hauke, and Debasish Banerjee, “Ground-state phase diagram of quantum link electrodynamics in $(2+1)$ -d,” *SciPost Phys.* **13**, 017 (2022).
- [72] Erez Zohar, J. Ignacio Cirac, and Benni Reznik, “Simulating $(2 + 1)$ -dimensional lattice qed with dynamical matter using ultracold atoms,” *Phys. Rev. Lett.* **110**, 055302 (2013).
- [73] R. Ott, T. V. Zache, F. Jendrzejewski, and J. Berges, “Scalable cold-atom quantum simulator for two-dimensional qed,” *Phys. Rev. Lett.* **127**, 130504 (2021).
- [74] Pierpaolo Fontana, Joao C. Pinto Barros, and Andrea Trombettoni, “Quantum simulator of link models using spinor dipolar ultracold atoms,” *Phys. Rev. A* **107**, 043312 (2023).
- [75] Federica Maria Surace, Pierre Fromholz, Nelson Darkwah Oppong, Marcello Dalmonte, and Monika Aidelsburger, “*ab initio* derivation of lattice gauge theory dynamics for cold gases in optical lattices,” (2023), [arXiv:2301.03474 \[cond-mat.quant-gas\]](https://arxiv.org/abs/2301.03474).
- [76] Jesse Osborne, Bing Yang, Ian P. McCulloch, Philipp Hauke, and Jad C. Halimeh, “Spin- s $U(1)$ quantum link models with dynamical matter on a quantum simulator,” (2023), [arXiv:2305.06368 \[cond-mat.quant-gas\]](https://arxiv.org/abs/2305.06368).
- [77] Jad C. Halimeh, Ian P. McCulloch, Bing Yang, and Philipp Hauke, “Tuning the topological θ -angle in cold-atom quantum simulators of gauge theories,” *PRX Quantum* **3**, 040316 (2022).
- [78] Yanting Cheng, Shang Liu, Wei Zheng, Pengfei Zhang, and Hui Zhai, “Tunable confinement-deconfinement transition in an ultracold-atom quantum simulator,” *PRX Quantum* **3**, 040317 (2022).
- [79] Jean-Yves Desaulles, Guo-Xian Su, Ian P. McCulloch, Bing Yang, Zlatko Papić, and Jad C. Halimeh, “Ergodicity Breaking Under Confinement in Cold-Atom Quantum Simulators,” *Quantum* **8**, 1274 (2024).
- [80] Thea Budde, Marina Krstić Marinković, and Joao C. Pinto Barros, “Quantum many-body scars for arbitrary integer spin in $2 + 1$ d abelian gauge theories,” (2024), [arXiv:2403.08892 \[hep-lat\]](https://arxiv.org/abs/2403.08892).

— Supplemental Material —
Quantum Many-Body Scarring in 2 + 1D Gauge Theories with Dynamical Matter
 Jesse Osborne, Ian P. McCulloch, and Jad C. Halimeh

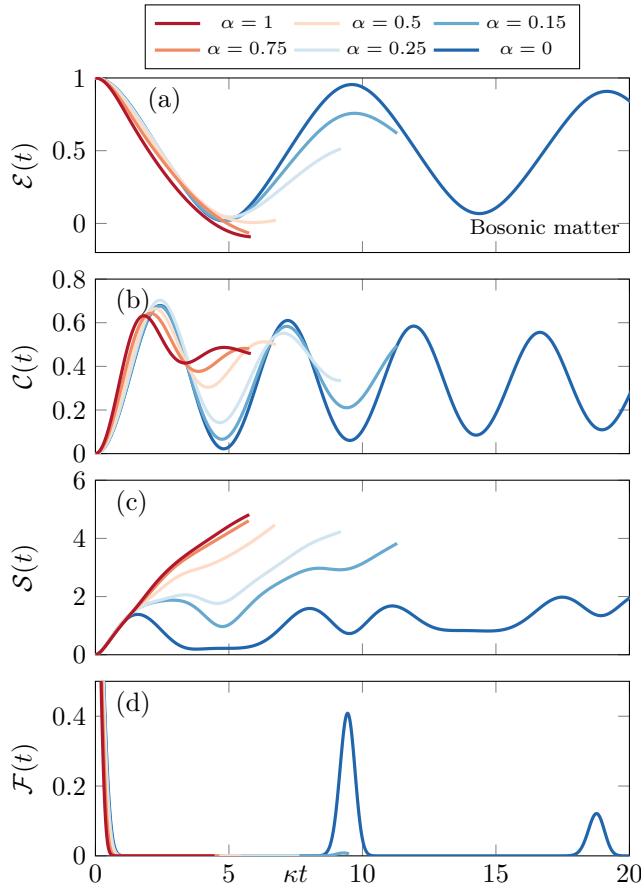


FIG. S1. A numerical time-evolution simulation of the quench of the vacuum state shown in Fig. 1(c) to $m = 0$, using matter with bosonic statistics on a $L_y = 4$ cylinder, as the coupling ratio α tuned from 1 to 0. (a) The flux $\mathcal{E}(t)$ (S1), (b) chiral condensate $\mathcal{C}(t)$ (3), and (c) entanglement entropy across a circumferential slice $\mathcal{S}(t)$, calculated for an infinite-length cylinder. (d) The fidelity $\mathcal{F}(t)$, calculated for a finite cylinder of dimension 4×16 with open boundaries in the x direction.

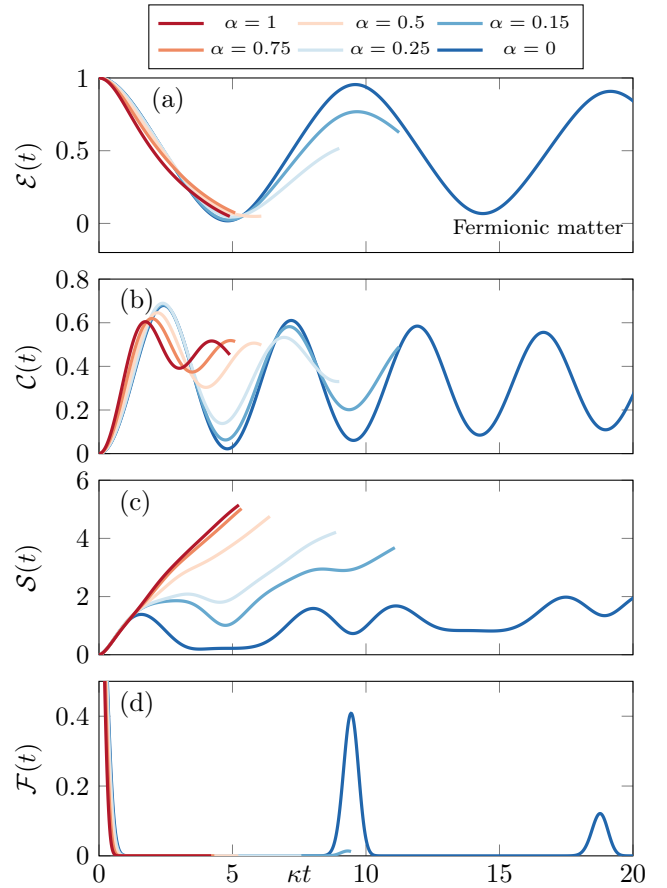


FIG. S2. A numerical time-evolution simulation of the quench of the vacuum state shown in Fig. 1(c) to $m = 0$, using matter with fermionic statistics on a $L_y = 4$ cylinder, as the coupling ratio α tuned from 1 to 0. (a) The flux $\mathcal{E}(t)$ (S1), (b) chiral condensate $\mathcal{C}(t)$ (3), and (c) entanglement entropy across a circumferential slice $\mathcal{S}(t)$, calculated for an infinite-length cylinder. (d) The fidelity $\mathcal{F}(t)$, calculated for a finite cylinder of dimension 4×16 with open boundaries in the x direction.

Quenches of the vacuum state

In Figures S1 and S2, we show quenches of a vacuum initial state (Fig. 1(c) in the main text) to $m = 0$. Here, we also show the expectation value of the electric flux $\mathcal{E}(t) = \langle \psi(t) | \hat{\mathcal{E}} | \psi(t) \rangle$,

$$\hat{\mathcal{E}} = \frac{1}{L_x L_y} \sum_{\mathbf{r}} \sum_{a=x,y} \hat{s}_{\mathbf{r}, \mathbf{e}_a}^z. \quad (\text{S1})$$

In the 1 + 1D case ($\alpha = 0$), this quench exhibits QMBS, but for $\alpha > 0$, the signs of QMBS are suppressed for both bosonic (Fig. S1) and fermionic (Fig. S2) matter fields, with little qualitative difference between the two different particle statistics.

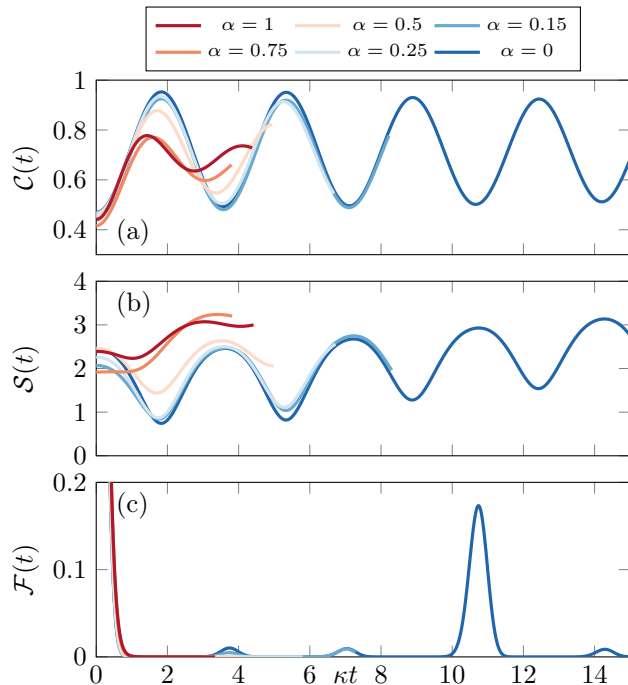


FIG. S3. A numerical time-evolution simulation of the quench of a gauge-invariant ground state at $m_i = 0.19\kappa$ to $m_f = -0.4\kappa$, using matter with bosonic statistics on a $L_y = 4$ cylinder, as the coupling ratio α tuned from 1 to 0. (a) The chiral condensate $\mathcal{C}(t)$ (3) and (b) entanglement entropy across a circumferential slice $\mathcal{S}(t)$, calculated for an infinite-length cylinder. (c) The fidelity $\mathcal{F}(t)$, calculated for a finite cylinder of dimension 4×16 with open boundaries in the x direction.

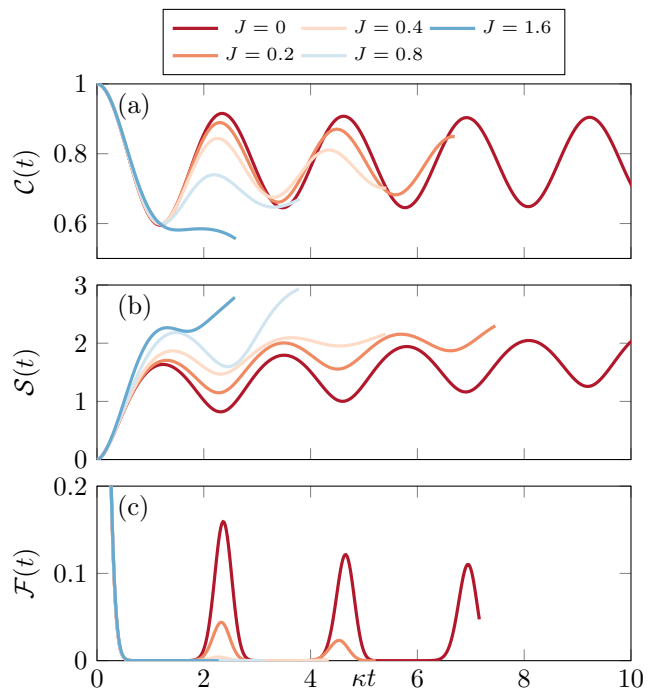


FIG. S4. A numerical time-evolution simulation of the quench of the charge-proliferated state shown in Fig. 1(b) to $m = 0.84\kappa$, using matter with bosonic statistics on a $L_y = 4$ cylinder, as the magnetic coupling J is increased, fixing the coupling ratio α to be 1. (a) The chiral condensate $\mathcal{C}(t)$ (3) and (b) entanglement entropy across a circumferential slice $\mathcal{S}(t)$, calculated for an infinite-length cylinder. (c) The fidelity $\mathcal{F}(t)$, calculated for a finite cylinder of dimension 4×16 with open boundaries in the x direction.

Quenches starting at a finite mass

Here, we examine a sudden quench from a finite value of the mass, starting with the gauge-invariant ground state at $m_i = 0.19\kappa$, and evolving the state at $m_f = -0.4\kappa$, which was shown to display strong signs of QMBS in the $1 + 1\text{D}$ model in Ref. [24]. As shown in Figure S3, however, for $\alpha > 0$ these signs are strongly suppressed. The way the gauge-invariant ground state at $m_i = 0.19\kappa$ changes as α is increased from zero to one would play a significant role here, and requires further investigation.

Effect of the magnetic coupling of the gauge fields

In Figure S4, we examine the effect of the magnetic coupling of the gauge fields, controlled by the plaquette term with coefficient J in the $2 + 1\text{D}$ QLM Hamiltonian, Eq. (1) in the main text. We look at the quench from the charge proliferated state (Fig. 1(b)) to $m = 0.84\kappa$ for bosonic matter, which was shown to display strong signs of QMBS in the main text (Fig. 2). However, for $J > 0$, we can see that these signs are quickly suppressed.